Crystalline-Symmetry-Protected Helical Majorana Modes in the Iron Pnictides

Elio J. König[1] and Piers Coleman[1,2]
[1]Department of Physics and Astronomy, Center for Materials Theory, Rutgers University, Piscataway, New Jersey 08854, USA
[2]Department of Physics, Royal Holloway, University of London, Egham, Surrey TW20 0EX, United Kingdom

(Received 10 February 2019; published 24 May 2019)

We propose that propagating one-dimensional Majorana fermions will develop in the vortex cores of certain iron-based superconductors, most notably $Li(Fe_{1-x}Co_x)As$. A key ingredient of this proposal is the 3D Dirac cones recently observed in photoemission experiments [P. Zhang *et al.*, Nat. Phys. **15**, 41 (2019)]. Using an effective Hamiltonian around the Γ-Z line we demonstrate the development of gapless one-dimensional helical Majorana modes, protected by C_4 symmetry. A topological index is derived which links the helical Majorana modes to the presence of monopoles in the Berry curvature of the normal state. We present various experimental consequences of this theory and discuss its possible connections with cosmic strings.

DOI: 10.1103/PhysRevLett.122.207001

Recent experimental [1–6] and theoretical [7–9] advances suggest that iron-based superconductors (FeSCs) can sustain fractionalized excitations. Building on these ideas, here we propose the emergence of dispersive, helical Majorana states in the flux phase of certain FeSCs.

Twelve years ago, two major discoveries occurred in condensed matter physics: the observation of high temperature superconductivity in the iron pnictides [10,11] and the discovery of topological insulators (TIs) [12]. FeSCs have challenged our understanding of strongly correlated electron materials, offering the possibility of practical applications. Topological insulators have transformed our understanding of band physics [13,14] and have led to the discovery of symmetry-protected Weyl and Dirac semimetals [15]. Remarkably, those materials emulate certain aspects of elementary particle physics in solid state experiments.

Yet despite the excitement in these two new fields, until recently, there has been little overlap between them. Iron-based superconductors are layered structures, in which d orbitals of the iron atoms form quasi-two-dimensional bands. The spin-orbit coupling (SOC) in the d bands was long thought to be too small for topological behavior. However, the recent discovery of marked spin-orbit splitting in photoemission spectra [16,17] has overturned this assumption, with an observation [1,7,8,17] that at small interlayer separations, an enhanced c-axis dispersion drives a topological band inversion between the iron d bands and ligand p_z orbitals. When the chemical potential lies in the hybridization gap between the d and p bands, the corresponding topological FeSCs sustain Majorana zero modes wherever magnetic flux lines intersect with the surface, Fig. 1(c). These excitations have been observed [3–6]. Here we demonstrate that on additional doping, topological behavior is expected to give rise to dispersive, helical Majorana fermions, Fig. 1(e), along the cores of superconducting vortices. Observation of these excitations would provide an important confirmation of the topological character of iron-based superconductors, yielding a new setting for the realization of Majorana fermions.

Helical Majorana fermions in one dimension correspond to a pair of gapless counterpropagating fermionic

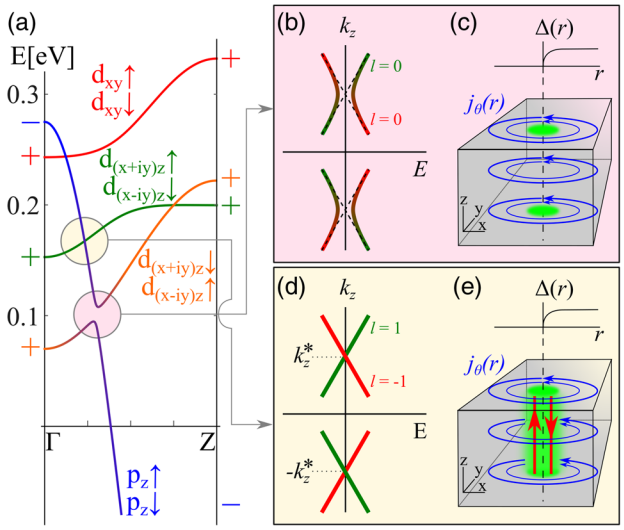

FIG. 1. Topology of FeSCs. (a) Band structure in the normal state. For small lattice spacing in c direction, p_z orbitals cross the d states along the Γ-Z line. When the chemical potential is near the spin-orbit induced gap (marked by a pink disk around 0.1 eV), the ground state is a topological superconductor. (b) In a vortex core, this implies a gapped dispersion of bulk Caroli–de Gennes–Matricon states with (c) Majorana zero modes (green pancakes) at the surface termination. At higher doping, when the Fermi energy lies in the vicinity of the Dirac node (marked by a yellow disk around 0.17 eV), (d),(e) C_4 symmetry protects helical Majorana states dispersing along the vortex cores.

TABLE I. Phases of matter which sustain $(1+1)$D helical or chiral Majorana fermions. We present all experimental evidence, the first material specific theoretical proposal, and generic classes of systems (in square brackets). We omitted Majorana modes which occur at fine-tuned critical points, e.g., at topological phase transitions [8,24] or at S-TI-S junctions with flux π [25]. Altland-Zirnbauer class (AZ cl.); experiment (Expt.); noncentrosymmetric superconductor (NCS); quantum anomalous Hall (QAH); quantum Hall (QH); superconductor (SC); superconducting semimetal (SSM).

	Boundary of 2D systems	Vortex in 3D system
Chiral	Expt.: QAH-SC [21], α-$RuCl_3$ [23], $\nu = 5/2$ QH [22] Theory: $p+ip$ SC [26] (Sr_2RuO_4 [27]?) [AZ cl. D [13]]	Expt.: Not observed Theory: TI-SC heterostructure [28] [Weyl SSM]
Helical	Expt.: Not observed Theory: NCS [29–32], $s_\pm$ SC + SOC [33] [AZ cl. DIII [13]	Expt.: Not observed Theory: ^{3}He-B [18], $LiFe_{1-x}Co_xAs$ (this work) [Dirac SSM]

excitations, first proposed as excitations within the "$o-$" vortices of superfluid ^{3}He-B [18]. While these excitations have not been observed, possibly because the energetics of ^{3}He-B favors less symmetric v vortices [19,20], which do not support helical Majorana modes, we here propose an alternative realization in FeSCs. Recent experimental advances (Table I) provide evidence for chiral (i.e., unidirectional) Majorana modes at the boundaries of various two-dimensional systems, including superconducting-quantum anomalous Hall heterostructures [21], 5/2 fractional quantum Hall states [22], and the layered Kitaev material α-$RuCl_3$ [23].

Majorana modes in FeSCs.—Here we summarize the main physics leading to the appearance of helical Majorana subgap states in the flux phase of FeSCs, when the magnetic field is aligned in the c direction. We shall concentrate on a case where the vortex core size (determined by the coherence length) is much larger than the lattice spacing, so that vortex-induced interpocket scattering can be neglected. This permits us to concentrate on the region of the Brillouin zone (BZ) which harbors the topological physics, in this case the Γ-Z line.

Along this line, the relevant electronic states are classified by the z component of their total angular momentum $J_z = L_z + S_z$. We may exploit the fact that the low-energy Hamiltonian close to the Γ-Z line [1,8,34] features an emergent continuous rotation symmetry. Three pairs of states are important, $|d_{(x+iy)z}\downarrow\rangle, |d_{(x-iy)z}\uparrow\rangle$ (with $j_z = \pm 1/2$), $|p_z,\uparrow\rangle, |p_z,\downarrow\rangle$ (also $j_z = \pm 1/2$), and $|d_{(x+iy)z}\uparrow\rangle, |d_{(x-iy)z}\downarrow\rangle$ ($j_z = \pm 3/2$). Their dispersion is shown in Fig. 1 along with the d_{xy} bands; we used the low-energy model of Ref. [8].

We briefly recapitulate the appearance of localized Majorana zero modes. The $j_z = \pm 1/2$ p_z states can hybridize with the corresponding $|d_{(x+iy)z}\downarrow\rangle, |d_{(x-iy)z}\uparrow\rangle$ states at intermediate k_z, leading to an avoided crossing of the bands [pink circle at 0.1 eV in Fig. 1(a)]. Since the p and d orbitals carry opposite parity, the band crossing leads to a parity inversion at the Z point. The system is therefore topological [35]. In the superconducting state, this system is then expected [25] to host topological surface superconductivity, developing localized Majorana zero modes at the surface termination of a vortex, Fig. 1(c). These Majorana zero modes can be alternatively interpreted as the topological end states of a fully gapped, 1D superconductor inside the vortex core [8]. In the bulk, where k_z is a good quantum number, the vortex hosts fermionic subgap states for each k_z near the normal state Fermi surface, Fig. 1(b). In particular, the lowest lying states carry angular momentum $l = 0$ and develop a topological hybridization gap upon inclusion of SOC.

However, bulk FeSCs can also support dispersive helical Majorana modes in their vortex cores. To see this, we now turn to the situation where the chemical potential lies near the Dirac cone, highlighted by a yellow circle at about 0.17 eV in Fig. 1(a). At this energy, semimetallic Dirac states are observed in ARPES (angle-resolved photoemission spectroscopy) [1]: these occur because the different j_z quantum numbers of $|p_z,\uparrow\rangle, |p_z,\downarrow\rangle$ and $|d_{(x+iy)z}\uparrow\rangle$, $|d_{(x-iy)z}\downarrow\rangle$ prevent a hybridization on the high symmetry line leading to a Hamiltonian of the (tilted) Dirac form $H(\boldsymbol{k}) = H_+(\boldsymbol{k}) \oplus H_-(\boldsymbol{k})$ [1,34],

$$H_\pm(\boldsymbol{k}) = \begin{pmatrix} M_p(k_z) & \pm v k_x + i v k_y \\ \pm v k_x - i v k_y & M_d(k_z) \end{pmatrix}, \qquad (1)$$

where $H_+(\boldsymbol{k})$ [$H_-(\boldsymbol{k})$] acts in the subspace of positive [negative] helicity spanned by $|p_z,\uparrow\rangle, |d_{(x+iy)z}\uparrow\rangle$ [$|p_z,\downarrow\rangle, |d_{(x-iy)z}\downarrow\rangle$]. The dispersion $M_p(k_z), M_d(k_z)$ of the relevant p and d orbitals is plotted in Fig. 1(a), and v is the transverse velocity.

We now assume that below T_c, a spin-singlet, s-wave superconducting phase develops. In an Abrikosov lattice of vortex lines, translational symmetry allows us to solve the problem at each k_z separately. At the particular values of $k_z = \pm k_z^*$, where $M_p(\pm k_z^*) = M_d(\pm k_z^*)$, H_+ and H_- separately take the form of a TI surface state. Consequently [25], for each helicity a nondegenerate Majorana zero mode appears in each vortex. Now, in contrast to the case of Fig. 1(b), these two modes carry different angular momenta $l = \pm 1$ so that they cannot be mixed by any perturbation which respects the C_4 symmetry. This leads to the gapless linear helical dispersion near $\pm k_z^*$.

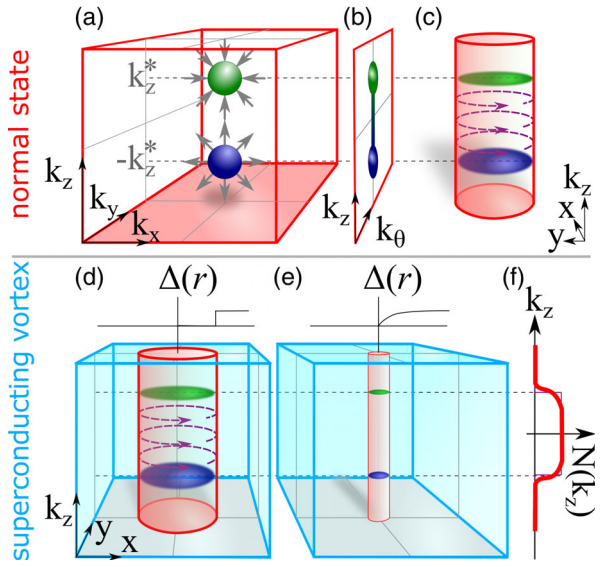

FIG. 2. Topological origin of helical Majorana modes. (a) Normal state BZ with helicity resolved Weyl nodes. (b) Surface BZ and Fermi arc. (c) Partial real space representation of a cylindrical Weyl semimetal. Fermi arc states (purple circles) terminate at topological transitions at $\pm k_z^*$ with delocalized, critical bulk states (green and blue pancakes). (d) A fat vortex: a normal state cylindrical core (red) embedded in a fully gapped superconductor (light blue). (e) A realistic thin vortex: Fermi arc states are finite size gapped, but the π Berry phase at $\pm k_z^*$ protects the critical states in the core [25,34]. (f) The index $N(k_z)$, Eq. (4) (purple, thin line), which we semiclassically relate to $\sigma_{xy}(k_z)$, Eq. (7) (red, thick line).

Topological origin of helical Majorana modes.—The crystalline topological protection of the helical Majorana modes in the flux phase of FeSCs can be understood as follows. First, we note that in the normal state, crystalline symmetries, in particular C_4, impose the decoupling of Hamiltonian Eq. (1) into the direct sum of two decoupled helical sectors. Within H_+ (H_-), two Weyl points of opposite topological charge ± 1 (∓ 1) appear at $(0, 0, \pm k_z^*)$, Fig. 2(a). Since crystalline symmetry ensures perfect decoupling, it is favorable to concentrate on a given sector in these explanations and superimpose both sectors in the end. The Berry flux connecting the two Weyl points implies a quantum anomalous Hall state for $k_z \in (-k_z^*, k_z^*)$ [36]. The resulting family of chiral edge states forms a Fermi arc in the surface BZ, Figs. 2(b) and 2(c). In view of their chiral nature, Fermi arc states can only terminate at a k_z which sustains critical bulk states—i.e., at the projection of the Weyl points. From the boundary perspective, their presence is ensured by the topological phase transition at $\pm k_z^*$.

We now turn to the superconducting case in the flux phase, for which a vortex core represents a normal state cylinder inside of a fully gapped superconducting background. At each $k_z \in (-k_z^*, k_z^*)$ the boundary of the vortex core resembles an interface between quantum anomalous Hall state and topological superconductor. This leads to a chiral Majorana encircling the cylinder—i.e., the Majorana analog [1,37] of Fermi arc states [purple circles, Fig. 2(d)]. As explained above, edge states may only disappear as a function of k_z when the bulk is critical; therefore, it follows that topologically protected vortex core subgap states must cross the Fermi energy at $\pm k_z^*$.

We conclude this discussion with three remarks. (1) For typical vortex core diameters ξ the chiral Majorana edge states are gapped by finite size effects, yet the above topological argument is still valid, Fig. 2(e). In particular, as in the case of a 3D TI surface, the magnetic flux prevents the critical bulk (i.e., vortex core) states at $\pm k_z^*$ from gapping. A different situation occurs in ^{3}He-A, where the conservation of the spin projection protects the nondispersive Fermi arc states for all k_z between the projection of Weyl points [20,34,38]. (2) Taking into account that H_+ and H_- sectors have opposite helicity, the actual state for $k_z \in (-k_z^*, k_z^*)$ is a quantum spin Hall insulator, and Fermi arc states are helical rather than chiral. (3) For weak misalignment of the flux line and the c axis, mixing between decoupled helical sectors $H_\pm$ is negligible. Under this assumption, the topological protection of helical modes persists.

Bogoliubov–de Gennes (BdG) Hamiltonian.—To confirm these heuristic arguments, we have perturbatively diagonalized [34] the BdG Hamiltonian of a topological FeSC with a single vortex. Here, we concentrate on states near k_z^* and employ a simplified Hamiltonian $\mathcal{H} = \mathcal{H}_+ \oplus \mathcal{H}_-$, where

$$\mathcal{H}_\pm = (H_\pm - \mu)\tau_z + \Delta(\boldsymbol{r})\tau_+ + \Delta^*(\boldsymbol{r})\tau_-. \tag{2}$$

The Fermi energy μ is measured from the Dirac point, $\Delta(\boldsymbol{r}) = |\Delta(r)|e^{i\theta}$ is the superconducting gap ($|\Delta(\infty)| \equiv \Delta$), $\tau_{x,y,z}$ are Pauli matrices in Nambu space, and $\tau_\pm = (\tau_x \pm i\tau_y)/2$. Assuming circularly symmetric vortices, we expand the wave function in angular momenta, seeking solutions of the form $\Psi_\pm = \sum_l e^{ik_z z + il\theta} U_\pm(\theta)\Psi_\pm^{(l)}(r, k_z)$, where the precise form of the diagonal matrices $U_\pm(\theta)$ is given in Supplemental Material [34]. At $l = \pm 1$ a chiral symmetry in the lth sector $\mathcal{H}_\pm^{(l)}$ allows us to explicitly construct an unpaired zero energy solution $\Psi_\pm^{(\pm 1)}(r, k_z^*)$ in each helical sector. We use these solutions to perturbatively include momenta $k_z - k_z^*$, a Zeeman field $g\mu_B B/2$, and orbital dependent gaps $\Delta_p - \Delta_d = \delta\Delta \neq 0$. By projecting onto the low-energy space, we obtain the effective dispersions

$$E_\pm(k_z) = \pm[v_M(k_z - k_z^*) - w_M\delta\Delta + g\mu_B B/2]. \tag{3}$$

This confirms the heuristic argument for the appearance of helical Majorana modes and demonstrates that perturbations merely shift k_z^*. A similar result holds near $-k_z^*$, so that in total two pairs of helical Majorana modes occur,

Fig. 1(d). In the limit $\mu \gg \Delta$ we obtain $v_M \sim \Delta^2 \partial_{k_z^*}[M_d(k_z^*) - M_p(k_z^*)]/\mu^2$ and $w_M \sim \Delta/\mu$. The velocity of helical Majorana modes in vortices of ^{3}He-B has an analogous parametrical dependence [18].

Index theorem.—We now demonstrate the link between the helical Majorana modes and the Berry flux between the two pairs of Weyl points, Fig. 2. While several topological invariants were proposed [39–42] to describe dispersive Majorana modes, we here employ a generalization of an index introduced by Volovik [43] for vortices in ^{3}He. Our index measures the imbalance between the number of states of opposite helicity at a given momentum k_z, $N(k_z) = [N_-(k_z) - N_+(k_z)]/2$, where

$$N_\pm(k_z) = \sum_n \theta[-E_n^\pm(k_z)] = \mathrm{Im}\int_{-\infty}^0 \frac{d\omega}{\pi}\mathrm{Tr}[\mathcal{G}_\pm(\omega - i0)]e^{\omega 0^+} \tag{4}$$

counts the number of states with given helicity in the Fermi sea ($\mathcal{G}_\pm(z) = [z - \mathcal{H}_\pm(k_z)]^{-1}$ and n labels quantum numbers. In a fully gapped system $N(k_z)$ is constant as a function of k_z. In contrast, the presence of helical Majorana modes, Fig. 1(d), implies a jump $N(k_z^* + 0^+) - N(k_z^* - 0^-) = 1$.

We now relate $N(k_z)$ to the quantized spin Hall conductivity at a given k_z using a semiclassical expansion, which is valid for smoothly varying $\Delta(\boldsymbol{r})$. In the eigenbasis of the normal state Hamiltonian $H_\pm(\boldsymbol{p})|u_{\boldsymbol{p},\xi,\pm}\rangle = \epsilon_{\xi,\pm}(\boldsymbol{p})|u_{\boldsymbol{p},\xi,\pm}\rangle$, the BdG Hamiltonian in each band takes the form $\mathcal{H}_{\xi,\pm} = \boldsymbol{d}_{\xi,\pm}\cdot\boldsymbol{\tau}$ (where the transverse components of $\boldsymbol{d}$ describe intraorbital pairing). In the following argument, we drop the band and helicity indices ξ and $\pm$ and employ a Wigner transform [34,44] so that $\boldsymbol{d}(\boldsymbol{R},\boldsymbol{P}) = [\mathrm{Re}\Delta(\boldsymbol{R}), -\mathrm{Im}\Delta(\boldsymbol{R}), \epsilon(\boldsymbol{P}) - \mu]$. Because of the algebra of Pauli matrices, the Green function $\mathcal{G}(\omega;\boldsymbol{R},\boldsymbol{P}) = [\omega - \boldsymbol{d}\cdot\boldsymbol{\tau}]^{-1}$ contains a commutator of operator convolutions (denoted by $\circ$):

$$\mathcal{G}(\omega;\boldsymbol{R},\boldsymbol{P}) = (\omega + \boldsymbol{d}\cdot\tau)\circ\left(\omega^2 - \boldsymbol{d}^2 - \frac{i}{2}\epsilon_{abc}[d_a\overset{\circ}{,}d_b]\tau_c\right)^{-1}. \tag{5}$$

The gradient expansion of the convolution is

$$[d_a\overset{\circ}{,}d_b](\boldsymbol{R},\boldsymbol{P}) \simeq i(\vec{\nabla}_X d_a\cdot\vec{\nabla}_P d_b - \vec{\nabla}_P d_a\cdot\vec{\nabla}_X d_b) + i\Omega_z\hat{e}_z\cdot(\vec{\nabla}_X d_a\times\vec{\nabla}_X d_b). \tag{6}$$

Here, $\Omega_z = i\langle\partial_{p_x}u_{\boldsymbol{p}}|\partial_{p_y}u_{\boldsymbol{p}}\rangle - i\langle\partial_{p_y}u_{\boldsymbol{p}}|\partial_{p_x}u_{\boldsymbol{p}}\rangle$ is the Berry curvature. Note that within our gauge invariant formalism, the semiclassical coordinates $\boldsymbol{R}$, $\boldsymbol{P}$ are *kinematic*—this leads to the appearance of Ω_z in addition to the Poisson bracket [45].

We evaluate $N(k_z)$ for an isotropic vortex of winding ν_v to leading order in gradients. The vortex enters Eq. (6) as $\vec{\nabla}_X d_y\times\vec{\nabla}_X d_x = \nu_v\hat{e}_z[\partial_R|\Delta(R)|^2]/2R$. Performing the radial integration and restoring the band and helicity indices leads to the result $N_\pm(k_z) = -\nu_v\sigma_{xy,\pm}(k_z)$, where

$$\sigma_{xy}^\pm(k_z) = \sum_\xi\int\frac{dk_x dk_y}{2\pi}\Omega_z^{\xi,\pm}(\boldsymbol{k})\theta(-\epsilon_{\xi,\pm}(\boldsymbol{k})). \tag{7}$$

In this expression, $\Omega_z^{\xi,\pm}(\boldsymbol{k})$ and $\epsilon_{\xi,\pm}$ are evaluated in the plane at constant k_z. It follows that $N(k_z) = \nu_v[\sigma_{xy}^+(k_z) - \sigma_{xy}^-(k_z)]/2$ is given by the normal state spin Hall conductivity which establishes the topological origin of the jump in the Fermi surface volume, Fig. 2(f).

Experimental realization.—We now summarize the topological features of iron-based superconductors observed to date. Topological Dirac surface states have been detected in $\mathrm{Fe}(\mathrm{Te}_x\mathrm{Se}_{1-x})$ and $\mathrm{Li}(\mathrm{Fe}_{1-x}\mathrm{Co}_x)\mathrm{As}$ using (S)ARPES, both in the normal and superconducting states [2], while photoemission evidence for 3D Dirac semimetallic bulk states in the normal state was also reported in Ref. [1]. Moreover, zero bias peaks in vortices of the flux phase of $\mathrm{Fe}(\mathrm{Te}_x\mathrm{Se}_{1-x})$ [3,5,6] and $(\mathrm{Li}_{1-x}\mathrm{Fe}_x)\mathrm{OHFeSe}$ [4] have been tentatively identified as Majorana bound states [see Fig. 1(c)]. However, the identification is still controversial, and other groups have questioned [46] whether the bound states are conventional Caroli–de Gennes–Matricon [47] states. Finally, a robust zero bias peak, akin to a Majorana bound state, was also reported to occur at excess iron atoms of FeTe [48]—an effect possibly due to trapped fluxes [49]. These experimental observations provide the foundation for our theoretical prediction of helical Majorana modes in the vortex cores of FeSC Dirac semimetals. Moreover, a successful experimental observation of helical Majorana modes in FeSCs could be used as independent experimental confirmation of the topological paradigm proposed for FeSCs.

$\mathrm{Li}(\mathrm{Fe}_{1-x}\mathrm{Co}_x)\mathrm{As}$, in which 3D bulk Dirac cones were observed in (S)ARPES at a doping level of $x = 0.09$ [1], is a strong candidate for these Majorana modes. It exhibits a $T_c(x = 0.09) \approx 9$ K [50] and, like all FeSCs, is a strongly type-II superconductor. To get an insight of typical experimental scales we compare to STM studies [51,52] of vortices in the parent compound LiFeAs (here, $T_c = 18$ K is larger but comparable). Vortices are observable at $B \geq 0.1$ T corresponding to typical vortex spacing of $l_B \lesssim 80$ nm, while the core radius is $\xi \approx 2.5$ nm. Therefore, intervortex tunneling, which would gap [53] the zero modes, is expected to be weak. Furthermore, the large ratio $\Delta/E_F \sim 0.5, \ldots, 1$ implies that the helical Majorana band should be well separated in energy from conventional Caroli–de Gennes–Matricon states [47].

A pair of helical Majorana modes displays universal thermal conductivity of $\kappa_0 = \mathcal{L}Te^2/h$, where $\mathcal{L} = \pi^2 k_B^2/3e^2$ is the Lorenz number [54], and the observation of this linear thermal conductivity is a key prediction of our theory. In the flux phase, each of the Φ/Φ_0 vortices hosts two pairs of

Majorana modes, so that the linear magnetic field dependence $\kappa_{\mathrm{tot}} = 2\kappa_0\Phi/\Phi_0$ of the total heat transport along the magnetic field direction can be easily discriminated from the phonon background. A similar effect occurs in the specific heat $C = 2c_0\Phi/\Phi_0$, with $c_0 = \pi k_B^2 T/3v_M$. Furthermore, STM measurements are expected to detect a spatially localized signal in the center of the vortex, with nearly constant energy dependence of the tunneling density of states $\nu(E) \overset{E\to 0}{\simeq} 1/\pi v_M$.

Summary and outlook.—In conclusion, we have demonstrated that propagating Majorana modes are expected to develop in the vortex cores of iron-based superconductors; see Fig. 1(e). These states are protected by crystalline C_4 symmetry, but generic topological considerations; Fig. 2 and Eq. (7) suggest they will be robust against weak misalignments. A key signature of these gapless excitations would be a dependence of various thermodynamic and transport observables on the density of vortices and magnetic field.

We conclude with an interesting connection which derives from the close analogy between superconducting and superfluid vortices and cosmic strings [20]: line defects thought to be formed in the early universe in response to spontaneous symmetry breaking of a grand unified field theory. Defects capable of trapping dispersive fermionic zero modes [55] may occur in speculative SO(10) grand unified theories but also in standard electroweak theory [56,57], and in either case the interaction of cosmic strings with magnetic fields leads to a sizable baryogenesis. Helical Majorana modes in the vortex of FeSCs may permit an experimental platform for testing these ideas.

We are grateful for discussions with P. Y. Chang, H. Ding, V. Drouin-Touchette, Y. Komijani, P. Kotetes, M. Scheurer, and P. Volkov. This work was supported by the U.S. Department of Energy (DOE), Office of Basic Energy Sciences (BES), under Award No. DE-FG02-99ER45790 (E. J. K. and P. C.), and by a QuantEmX travel grant (E. J. K.) from the Institute for Complex Adaptive Matter and the Gordon and Betty Moore Foundation through Grant No. GBMF5305.

Note added in proof.—Recently, two articles [58,59] appeared and present consistent results on $(1+1)$D Majorana modes in vortices of FeSCs. Experimental signatures of helical Majorana fermions were reported in Refs. [60,61].

[1] P. Zhang *et al.*, Nat. Phys. **15**, 41 (2019).
[2] P. Zhang, K. Yaji, T. Hashimoto, Y. Ota, T. Kondo, K. Okazaki, Z. Wang, J. Wen, G. D. Gu, H. Ding, and S. Shin, Science **360**, 182 (2018).
[3] D. Wang, L. Kong, P. Fan, H. Chen, S. Zhu, W. Liu, L. Cao, Y. Sun, S. Du, J. Schneeloch, R. Zhong, G. Gu, L. Fu, H. Ding, and H.-J. Gao, Science **362**, 333 (2018).
[4] Q. Liu, C. Chen, T. Zhang, R. Peng, Y.-J. Yan, C.-H.-P. Wen, X. Lou, Y.-L. Huang, J.-P. Tian, X.-L. Dong, G.-W. Wang, W.-C. Bao, Q.-H. Wang, Z.-P. Yin, Z.-X. Zhao, and D.-L. Feng, Phys. Rev. X **8**, 041056 (2018).
[5] T. Machida, Y. Sun, S. Pyon, S. Takeda, Y. Kohsaka, T. Hanaguri, T. Sasagawa, and T. Tamegai, arXiv:1812.08995.
[6] L. Kong, S. Zhu, M. Papaj, L. Cao, H. Isobe, W. Liu, D. Wang, P. Fan, H. Chen, Y. Sun, S. Du, J. Schneeloch, R. Zhong, G. Gu, L. Fu, H.-J. Gao, and H. Ding, arXiv:1901.02293.
[7] Z. Wang, P. Zhang, G. Xu, L. K. Zeng, H. Miao, X. Xu, T. Qian, H. Weng, P. Richard, A. V. Fedorov, H. Ding, X. Dai, and Z. Fang, Phys. Rev. B **92**, 115119 (2015).
[8] G. Xu, B. Lian, P. Tang, X.-L. Qi, and S.-C. Zhang, Phys. Rev. Lett. **117**, 047001 (2016).
[9] R. Zhang, W. Cole, and S. Das Sarma, Phys. Rev. Lett. **122**, 187001 (2019).
[10] Y. Kamihara, H. Hiramatsu, M. Hirano, R. Kawamura, H. Yanagi, T. Kamiya, and H. Hosono, J. Am. Chem. Soc. **128**, 10012 (2006).
[11] H. Takahashi, K. Igawa, K. Arii, Y. Kamihara, M. Hirano, and H. Hosono, Nature (London) **453**, 376 (2008).
[12] M. König, S. Wiedmann, C. Brüne, A. Roth, H. Buhmann, L. W. Molenkamp, X.-L. Qi, and S.-C. Zhang, Science **318**, 766 (2007).
[13] A. P. Schnyder, S. Ryu, A. Furusaki, and A. W. W. Ludwig, Phys. Rev. B **78**, 195125 (2008).
[14] B. Bernevig and T. Hughes, *Topological Insulators and Topological Superconductors* (Princeton University Press, Princeton, New Jersey, 2013).
[15] N. P. Armitage, E. J. Mele, and A. Vishwanath, Rev. Mod. Phys. **90**, 015001 (2018).
[16] P. D. Johnson, H.-B. Yang, J. D. Rameau, G. D. Gu, Z.-H. Pan, T. Valla, M. Weinert, and A. V. Fedorov, Phys. Rev. Lett. **114**, 167001 (2015).
[17] S. V. Borisenko, D. V. Evtushinsky, Z. H. Liu, I. Morozov, R. Kappenberger, S. Wurmehl, B. Büchner, A. N. Yaresko, T. K. Kim, M. Hoesch, T. Wolf, and N. D. Zhigadlo, Nat. Phys. **12**, 311 (2016).
[18] T. S. Misirpashaev and G. Volovik, Phys. B **210**, 338 (1995).
[19] D. Vollhardt and P. Wölfle, *The Superfluid Phases of Helium 3*, (Taylor and Francis, London, England, 1990).
[20] G. Volovik, *The Universe in a Helium Droplet*, International Series of Monographs on Physics (Clarendon Press, Oxford, England, 2003).
[21] Q. L. He, L. Pan, A. L. Stern, E. C. Burks, X. Che, G. Yin, J. Wang, B. Lian, Q. Zhou, E. S. Choi, K. Murata, X. Kou, Z. Chen, T. Nie, Q. Shao, Y. Fan, S.-C. Zhang, K. Liu, J. Xia, and K. L. Wang, Science **357**, 294 (2017).
[22] M. Banerjee, M. Heiblum, V. Umansky, D. E. Feldman, Y. Oreg, and A. Stern, Nature (London) **559**, 205 (2018).
[23] Y. Kasahara, T. Ohnishi, Y. Mizukami, O. Tanaka, S. Ma, K. Sugii, N. Kurita, H. Tanaka, J. Nasu, Y. Motome *et al.*, Nature (London) **559**, 227 (2018).
[24] P. Hosur, P. Ghaemi, R. S. K. Mong, and A. Vishwanath, Phys. Rev. Lett. **107**, 097001 (2011).
[25] L. Fu and C. L. Kane, Phys. Rev. Lett. **100**, 096407 (2008).

[26] G. E. Volovik, Zh. Eksp. Teor. Fiz. **94**, 123 (1988) [Sov. Phys. JETP **67**, 1804 (1988)].
[27] T. M. Rice and M. Sigrist, J. Phys. Condens. Matter **7**, L643 (1995).
[28] T. Meng and L. Balents, Phys. Rev. B **86**, 054504 (2012).
[29] Y. Tanaka, T. Yokoyama, A. V. Balatsky, and N. Nagaosa, Phys. Rev. B **79**, 060505(R) (2009).
[30] M. Sato and S. Fujimoto, Phys. Rev. B **79**, 094504 (2009).
[31] R. Roy, arXiv:0803.2868.
[32] X.-L. Qi, T. L. Hughes, S. Raghu, and S.-C. Zhang, Phys. Rev. Lett. **102**, 187001 (2009).
[33] F. Zhang, C. L. Kane, and E. J. Mele, Phys. Rev. Lett. **111**, 056402 (2013).
[34] See Supplemental Material at http://link.aps.org/supplemental/10.1103/PhysRevLett.122.207001 for a perturbative solution near $\pm k_z^*$, a derivation of the index theorem and a quasiclassical calculation.
[35] L. Fu and C. L. Kane, Phys. Rev. B **76**, 045302 (2007).
[36] Strictly speaking, if k_z states are filled up to a finite Fermi momentum k_F around the Weyl node, quantization occurs for the smaller interval $k_z \in (-k_z^* + k_F, k_z^* - k_F)$.
[37] S. A. Yang, H. Pan, and F. Zhang, Phys. Rev. Lett. **113**, 046401 (2014).
[38] G. E. Volovik, JETP Lett. **93**, 66 (2011).
[39] E. J. Weinberg, Phys. Rev. D **24**, 2669 (1981).
[40] J. C. Y. Teo and C. L. Kane, Phys. Rev. B **82**, 115120 (2010).
[41] X.-L. Qi, E. Witten, and S.-C. Zhang, Phys. Rev. B **87**, 134519 (2013).
[42] B. Roy and P. Goswami, Phys. Rev. B **89**, 144507 (2014).
[43] G. Volovik, JETP Lett.Pis'ma Zh. Eksp. Teor. Fiz. **49**, 343 (1989); [JETP Lett. **49**, 391 (1989)].
[44] E. König and A. Levchenko (unpublished).
[45] B. Al'tshuler, Zh. Eksp. Teor. Fiz. **75**, 1330 (1978) [Sov. Phys. JETP **48**, 670 (1978)].
[46] M. Chen, X. Chen, H. Yang, Z. Du, X. Zhu, E. Wang, and H.-H. Wen, Nat. Commun. **9**, 970 (2018).
[47] C. Caroli, P. G. De Gennes, and J. Matricon, Phys. Lett. **9**, 307 (1964).
[48] J.-X. Yin, Z. Wu, J.-H. Wang, Z.-Y. Ye, J. Gong, X.-Y. Hou, L. Shan, A. Li, X.-J. Liang, X.-X. Wu, J. Li, C.-S. Ting, Z.-Q. Wang, J.-P. Hu, P.-H. Hor, H. Ding, and S. H. Pan, Nat. Phys. **11**, 543 (2015).
[49] K. Jiang, X. Dai, and Z. Wang, Phys. Rev. X **9**, 011033 (2019).
[50] Y. M. Dai, H. Miao, L. Y. Xing, X. C. Wang, P. S. Wang, H. Xiao, T. Qian, P. Richard, X. G. Qiu, W. Yu, C. Q. Jin, Z. Wang, P. D. Johnson, C. C. Homes, and H. Ding, Phys. Rev. X **5**, 031035 (2015).
[51] T. Hanaguri, K. Kitagawa, K. Matsubayashi, Y. Mazaki, Y. Uwatoko, and H. Takagi, Phys. Rev. B **85**, 214505 (2012).
[52] S. S. Zhang, J.-X. Yin, G. Dai, H. Zheng, G. Chang, I. Belopolski, X. Wang, H. Lin, Z. Wang, C. Jin, and M. Z. Hasan, Phys. Rev. B **99**, 161103(R) (2019).
[53] T. Liu and M. Franz, Phys. Rev. B **92**, 134519 (2015).
[54] M. J. Pacholski, C. W. J. Beenakker, and I. Adagideli, Phys. Rev. Lett. **121**, 037701 (2018).
[55] R. Jackiw and P. Rossi, Nucl. Phys. **B190**, 681 (1981).
[56] A. Vilenkin and E. Shellard, *Cosmic Strings and Other Topological Defects*, Cambridge Monographs on Mathematical Physics (Cambridge University Press, Cambridge, England, 2000).
[57] E. Witten, Nucl. Phys. **B249**, 557 (1985).
[58] S. Qin, L. Hu, X. Wu, X. Dai, C. Fang, F.-C. Zhang, and J. Hu, arXiv:1901.03120.
[59] S. Qin, L. Hu, C. Le, J. Zeng, F.-C. Zhang, C. Fang, and J. Hu, arXiv:1901.04932.
[60] M. J. Gray *et al.*, arXiv:1902.10723.
[61] Z. Wang, J. Olivares Rodriguez, M. Graham, G. D. Gu, T. Hughes, D. K. Morr, and V. Madhavan, arXiv:1903.00515.